Chronic Exposure to PM2.5 Aggravates SLE Manifestations in Lupus-Prone Mice

Victor Yuji Yariwake (victor.yariwake@usp.br)
School of Medicine, University of São Paulo https://orcid.org/0000-0003-0639-1228

Janaína Iannicelli Torres
School of Medicine of University of São Paulo

Amandda Rakell Peixoto dos Santos
Federal University of São Paulo

Sarah Cristina Ferreira Freitas
Universidade Nove de Julho

Kátia De Angelis
Universidade Nove de Julho

Sylvia Costa Lima Farhat
School of Medicine of University of São Paulo

Niels Olsen Saraiva Câmara
Institute of Biomedical Sciences of University of São Paulo

Mariana Matera Veras
School of Medicine of University of São Paulo

Research

Keywords: Air pollution, Systemic lupus erythematosus, Particulate matter, Lupus nephritis, Autoimmunity, Environmental exposure

Posted Date: December 31st, 2020

DOI: https://doi.org/10.21203/rs.3.rs-137403/v1

Version of Record: A version of this preprint was published on March 25th, 2021. See the published version at https://doi.org/10.1186/s12989-021-00407-0.

Abstract

Background: Air pollution causes negative impacts on health. Systemic lupus erythematosus (SLE) is an autoimmune disease with diverse clinical manifestations and multifactorial etiology. Recent studies suggest that air pollution can trigger SLE and induce disease activity. However, this association has not been deeply investigated. Thus, the aim of this study was to evaluate whether exposure to fine particulate matter (PM2.5) exacerbates SLE manifestations, focusing on renal complications, in a lupus-prone animal model. Female NZBWF1 mice were exposed daily to 600μg/m³ of inhaled concentrated ambient particles (CAP) or filtered air (FA). Survival rate, body weight, weight of organs (kidney, spleen, thymus, liver and heart), blood cell count, proteinuria, kidney stereology, renal histopathology, gene expression and oxidative stress were analyzed.

Results: Female NZBW mice exposed to CAP presented decreased survival, increased circulating neutrophils, early onset of proteinuria and increased kidney weight with renal cortex enlargement when compared to NZBW mice exposed to FA.

Conclusions: This work shows that air pollution aggravates some SLE manifestations in lupus-prone mice. These results reinforce the need of reducing air pollutant levels in order to promote a better quality of life for individuals diagnosed with SLE.

Background

Systemic lupus erythematosus (SLE) is a complex autoimmune disease with diverse clinical manifestations. Skin, joints, blood and kidneys are the most affected by chronic inflammatory processes [1, 2]. SLE etiology remains not fully elucidated. However, genetic and environmental factors contribute to their development [3, 4]. Variations in HLA-DR (recognition of self and non-self-antigens) and type-I interferon genes are commonly reported among SLE patients [5, 6]. However, these genetic variations do not explain the increase of SLE incidence worldwide over the last decades [7]. Among environmental factors, UV radiation, viral infections (Epistein-Barr), drugs (procainamide and hidralazine), alcohol, tobacco and silica are considered risk factors associated with SLE development [8, 9].

Recently, epidemiological evidences suggest that exposure to air pollution could be a potential contributor for SLE activation and aggravation through systemic inflammation and oxidative stress [10, 11]. Air pollution is the major environmental risk for health; last reports from the World Health Organization (WHO) showed that annually more than 4 million deaths could be associated with exposure to ambient air pollution [12, 13]. Moreover, epi and experimental studies have demonstrated that exposures are associated with respiratory, cardiovascular, neurologic, endocrine and reproductive disorders [14, 15, 16].

Air pollutants comprise a mixture of gases, organic compounds, metals and particles suspended [17]. Within this mixture, fine particulate matter (PM2.5) is the pollutant with the strongest relationship with negative health outcomes and mortality [18, 19]. The process of fossil fuel combustion is the main source of PM2.5 generation and its small size facilitates penetration deeply into the respiratory system. Inhalation of these particles are associated with the promotion of local to systemic inflammatory processes and oxidative stress [20, 21].

Immunopathology of SLE comprises the production of autoantibodies, mainly against nuclear antigens, that form immune complexes (IC). These IC deposit in tissues and vessels amplifying inflammatory responses,

characterized by complement activation, recruitment of immune cells and tissue damage [22, 23]. Kidney complications are very common in SLE due to deposition of IC in glomeruli. Some patients can develop proteinuria, glomerulosclerosis and kidney failure depending on the disease gravity [22, 24]. Plausible mechanisms involved in the association of air pollution and lupus include: the systemic inflammatory response and oxidative stress triggered by particles in the lungs; alteration of TH1/TH2/TH17 cells ratio and activation of B cells and dendritic cells induced by the translocation of particles into the bloodstream; increased apoptosis and defective clearance of apoptotic debris stimulating autoimmunity; and epigenetic changes [10, 25, 26, 27].

Therefore, in this novel study we aimed to evaluate whether chronic exposure to PM2.5 exacerbates clinical manifestations of SLE (focusing on kidney and systemic involvement) on female mice spontaneously predisposed to SLE development (NZBWF1 strain). We investigated a murine model that mimics human condition to study disease progression in predisposed individuals for a better understanding of air pollution negative impacts on SLE.

Methods

Animals and experimental design: Female NZBWF1 mice, 75-day-old, were purchased from Jackson Laboratory (Bar Harbor, USA) and utilized as SLE model (n = 10). Female C57/Bl6 mice of the same age were obtained from University of Campinas and utilized as controls (n = 16). After 15 days of acclimatization, each strain was randomly subdivided into two groups, one exposed to filtered air (FA) and one exposed to concentrated ambient particles (CAP). In total, animals were divided into four groups: control mice exposed to FA (C57-FA) (n = 8); control mice exposed to CAP (C57-CAP) (n = 8); lupus-prone mice exposed to FA (NZBW-FA) (n = 10); lupus-prone mice exposed to CAP (NZBW-CAP) (n = 10). Exposure to FA or CAP occurred for four months (starting from 90-day-old until 210-day-old). During the exposure period, animals were weighed, and urine samples were collected monthly. Also, the health status of the animals was checked daily, and survival was evaluated. Experimental design is shown in Fig. 1. Animals were allocated in cages (4–5 animals/cage) lined with pine wood shavings, and cardboard tubes and cotton balls for nesting were used as environmental enrichment strategies. Food and water were provided *ad libitum*. Except during CAP exposures, cages were put into closed ventilated hacks supplied with HEPA filtered air, controlled temperature of 21–23ºC and under light/dark cycle of 12 h/12 h. Animal procedures were approved by the Ethical Committee for Animal Research (CEUA) of the School of Medicine of University of São Paulo (FMUSP), under protocol number 095/17.

Daily exposure to PM2.5

Animal exposure to PM2.5 was performed in the Harvard Ambient Particle Concentrator (HAPC), located at FMUSP (Sao Paulo, Brazil). Exposures were performed in whole-body inhalation chambers (CAP or FA) as described in previous studies [28, 29, 30]. Before the initiation of the exposures, animals were also acclimatized to the HAPC for 5 days to reduce the distress of handling. C57-FA and NZBW-FA groups were exposed only to FA. C57-CAP and NZBW-CAP groups were exposed daily to 600 μg/m³ of CAP. This concentration represents the adjusted air concentration that São Paulo residents are exposed to [30]. This adjusted air concentration ($C_{air-adj}$) of 600 μg/m³ in 1 day/24hs was determined following current methodology of Environmental Protection Agency (EPA) [31], as follows

$C_{air-adj} = C_{air}$ x ET x EF x ED/AT x 1 day/24 hours

Where:

C_{air} = Concentration of contaminant in air (mg/m^3) = 25 μg/m³ (São Paulo)

ET = Exposure time (hours/day) = 24 h/day

EF = Exposure frequency (days/year) = 365 days/year

ED = Exposure duration (years) = 1 year

AT = Averaging time (days) = 365 days

PM2.5 characterization

Samples of ambient PM2.5 were collected for characterization of PM2.5 elemental composition. For this, polycarbonate filter samples were coupled into Harvard Virtual Impactor (a device that permits only the passage of particles with diameter less than 2,5 μm) for 24hs. A flux of 10L/min was generated by a vacuum pump for retention of ambient PM2.5 in sample filters. Characterization of PM2.5 elemental composition was performed by energy dispersive X-ray spectroscopy (EDX) as previously described [32]. 20 filter samples were analyzed by EDX.

Proteinuria analysis: Isolated urine samples were collected monthly by stimulation of perineal area as previous described [33]. Protein/creatinine ratio (PCR) and albumin/creatinine ratio (ACR) of urine samples were assessed. Dosage of total proteinuria was performed using Sensiprot kit (Labtest Diagnosis, Brazil). Procedures were conducted according to the manufacturer. Samples were diluted at 1:5 and incubated with color reagent at 37ºC/5 min. Absorbance was read at wavelength 600 nm. Quantification of proteinuria (mg/dL) was determined based on the absorbance of the sample (A_{sa}) and standard (A_{st}) through the equation "[(A_{sa} ÷ A_{st}) x 50] x 5", where 50 corresponds to the protein standard concentration in mg/dL and 5 to the dilution factor. Dosage of creatininuria was performed following modified Jaffe method (Labtest Diagnosis, Brazil). Samples were diluted at 1:125 and incubated with a solution of 80% picric acid, 1% m/v + 20% sodium hydroxide, 10% m/v at 25ºC/20 min. Absorbance was read at wavelength 520 nm. Quantification of creatininuria (mg/dL) was determined based on the absorbance of the sample (A_{sa}) and standard (A_{st}) through the equation "[(A_{sa}) ÷ (A_{st}) x 5] x 25", where 5 corresponds to the standard concentration in mg/dL and 25 to the dilution factor (1:125) corrected by the creatinine standard concentration (5 mg/dL). Albuminuria quantification was performed using electrophoresis gel. Firstly, urine samples were treated with laemmli buffer (5% β-mercaptoethanol) and heat (95ºC/5 min) for protein denaturation. Proteins were run on a 10% SDS-polyacrylamide electrophoresis gel and stained with Coomassie Blue R-259. After the staining, gels were immersed in a destain solution (7.5% acetic acid + 25% methanol + 67.5% distilled water) and gel images were obtained from Amersham Imager 600 (GE Healthcare, USA). Quantification of albuminuria (μg/mL) was performed by ImageJ software (Media Cybernetics, USA). Briefly, stained albumin in the samples was observed in bands at 66.5 kDa and the pixels of each band were measured and compared to a standard band (corresponding to 125 μg/mL of BSA). Note that for each gel there was a standard band control. Then, albuminuria were normalized by their creatinine concentration previously measured in the respective urine samples.

Euthanasia procedures

Animals were euthanized right after the fourth month of exposure (at 210 day-old) through overdose inhalation of the anesthetic isoflurane (Cristalia, Brazil). Blood samples were collected for hemogram and serologic analyses. Kidneys, spleen, liver, heart and thymus were collected, weighed and stored for histological and molecular analyses.

Hemogram analysis

Complete blood count was performed for blood cells screening. Red blood cells, white blood cells (including total count and percentage of neutrophils, eosinophils, basophils, monocytes and lymphocytes) and platelets were counted. Analysis was conducted using the automated hematologic counter pocH 100iV (Sysmex, Brazil).

Anti-DNA quantification: Blood samples were centrifuged (3500 rpm/10 min) for plasma collection. Quantification of anti-DNA antibodies was performed by indirect immunofluorescence using NOVA Lite® dsDNA Crithidia luciliae kit (Inova Diagnostics, USA) following manufacturer protocol. Goat anti-Mouse IgG (H + L) Cross-Adsorbed Secondary Antibody, Alexa Fluor 488 (Invitrogen, A-11001) was utilized at 1:100 for conjugation.

Histological analyses of kidneys

After euthanasia, kidneys were stored in buffered formaldehyde (10%) for 24hs. Then, kidneys were processed and embedded in paraffin. For stereological analysis kidneys were sliced (5 μm thick) in seriated sections spaced by 100 μm and stained with hematoxylin-eosin (HE). In the interval between serial sections, sets of sections were collected for immunohistochemistry and histopathology. HE slides were scanned and digitalized using Pannoramic SCAN (3DHistech, Hungary). Volume estimation of kidney compartments was determined using Cavalieri method [34]. Using ImageJ software (Media Cybernetics, USA), a grid was superposed over the digitalized images (x10 magnification) and the incident points were counted. Relative volumes of cortex and medulla were calculated by dividing the sum of incident points of each compartment by the sum of total points of the kidney. Absolute volumes of compartments were calculated by multiplying relative volumes by total kidney volume. Total kidney volume was estimated by dividing kidney weight by kidney density (d = 1,06 g/cm³). For histopathologic analysis kidneys slices were randomly selected and stained using Periodic acid-Schiff (PAS). PAS slides were scanned and digitalized as previously described. Case viewer software (3DHistech, Hungary) was utilized for quantification (attribution of histopathological scores [35]) of tubular and glomerular alterations (x400 magnification) and for estimation of glomerular volume by measuring average diameter of glomeruli [36]. For analysis of collagen deposition another set of randomly selected were stained by picrosirius-hematoxylin method [37]. Slides were scanned and digitalized as previously described. Ten pictures per animal were taken. Threshold tool of ImageJ software (Media Cybernetics, USA) was utilized for estimation of the area stained with picrosirius (x100 magnification).

Immunohistochemistry: Immunohistochemistry protocol followed the manufacturer instructions. Briefly, sections were hydrated, antigen retrieval was performed in sodium citrate buffer (pH = 6) at 96ºC/20 min, endogen peroxidase was blocked with methanol (95%) + peroxide hydrogen (5%) for 30 min and non-specific bounds were blocked with bovine serum albumin (2%) for 60 min. Then we incubated sections with primary antibodies anti-C3 (1:2000 - ab200999), anti-IgG (1:250 - ab190475) and macrophage marker (1:10 - sc-101447) at 4ºC/overnight. Next, slices were incubated with HRP-polymer anti-rabbit (ab214880) or HRP-polymer anti-rat (ab214882) for 90 min and the chromogen 3,3'-diaminobenzidine (DAB) was added. Counterstaining was performed with hematoxylin. Slides were scanned and digitalized as described previously. Ten pictures per

animal were taken. Threshold tool of ImageJ software (Media Cybernetics, USA) was utilized for estimation of area stained with DAB (x100 magnification).

Gene expression

Total RNA from kidneys was extracted with Trizol reagent (Invitrogen, USA). Kidneys were immersed in trizol and macerated in Precellys (Bertin Instruments, France). Chloroform was added, the homogenate was centrifuged, and the supernatant (RNA) was collected. RNA precipitation was performed with isopropanol. After centrifugation RNA pellet was washed with ethanol 70% twice and diluted in DEPC H_2O. Quantification of total RNA (ng/µL) and quality of extraction (260/230) was performed using Nanodrop (Thermo Scientific, USA). Synthesis of cDNA was performed with 2000 ng of total RNA. First step was the degradation of contaminant DNA with RNAase-free DNase (Promega, USA). Second step was the addition of oligo-dT (Promega, USA). Last step was the reaction with dNTP and M-MLV Reverse Transcriptase (Promega, USA). All steps were performed in Mastercycler (Eppendorf, Germany). Relative gene expression of NFκB and TGF-β was determined by quantitative real-time PCR following $2^{-\Delta\Delta CT}$ method [38]. HPRT was utilized as endogenous gene (Additional file 1). For each gene, 4 µL cDNA sample + 0,5 µL forward primer + 0,5 µL reverse primer + 5 µL mastermix SYBR (Invitrogen, USA) were assembled. Samples were run in duplicates. qRT-PCR was performed at Quantstudio 12K Flex (Applied Biosystems, USA).

Oxidative stress

Pro-oxidant (NADPH oxidase and hydrogen peroxide) and antioxidant (FRAP) assays were performed for oxidative stress analysis of kidneys following procedures described elsewhere [39]. Firstly, kidneys were homogenized in an Ultra80 Turrax Blender (UltraStirrer, Switzerland) with 120 mM KCl and 20 nM sodium phosphate buffer (1 g tissue/4 mL solution) and centrifuged at 600 rpm/10 min. Activity of NADPH oxidase enzyme was determined by ELISA based on superoxide anion production [40]. The assay was performed with 50 mM phosphate buffer containing 2 mM EDTA and 150 mM sucrose, 1.3 mM NADPH and 10 µL of homogenate samples. Superoxide production was determined using a spectrometer (SpectraMax2, Molecular Devices) at 340 nm wavelength. Hydrogen peroxide dosage was determined by oxidation of phenol red by radish peroxidase [41]. 70 µL of homogenate samples were added in 180 µL of radish peroxidase solution (dextrose buffer + phenol red + radish peroxidase type II). After 25 min of incubation, 5 µL of sodium hydroxide were added to stop the reaction and absorbance was determined in a spectrometer (SpectraMax2, Molecular Devices) at 630 nm wavelength. Non-enzymatic antioxidant activity was determined by ferric reducing antioxidant power (FRAP) [42]. 10 µL of homogenate samples were added in 290 µL of FRAP reactive (sodium acetate and acetic acid buffer + 10 mM TPTZ + 20 mM hexahydrate ferric chloride). After 5 min of incubation, absorbance was determined in a spectrometer (SpectraMax2, Molecular Devices) at 593 nm wavelength.

Statistical analyses

SPSS software version 17.0 (IBM, USA) was utilized for statistical analyses. Firstly, descriptive data were obtained, and normality was verified by Kolmogorov-Smirnov test. Variables with normal distribution were analyzed through the parametric test ANOVA and post-hoc tests of Tukey HSD, Gabriel or Games Howell. Test-T was performed for comparison between 2 groups. Variables with non-normal distribution were ranked and analyzed through ANOVA. Kruskal-Wallis (4 groups) and Mann-Whitey test (2 groups) were also applied for non-

normal parameters. Survival analysis was performed with Kepler-Maier test. Differences between groups were considered statistically significant when p value was less than 0.05 ($p < 0.05$).

Results

PM2.5 characterization

Elemental composition of ambient PM2.5 is presented in Table 1.

Table 1
Elemental composition of PM2.5.

Element	%
Carbon (C)	52.24 ± 6.24
Sulphur (S)	33.59 ± 2.11
Magnesium (Mg)	10.19 ± 8.56
Barium (Ba)	1.34 ± 0.47
Chloride (Cl)	1.00 ± 0.28
Phosphorus (P)	0.73 ± 0.42
Iron (Fe)	0.34 ± 0.13
Calcium (Ca)	0.28 ± 0.09
Potassium (K)	0.15 ± 0.03
Silicon (Si)	0.04 ± 0.07
Bars represent percentage mean ± error. n = 20 filters.	

Survival analysis

Four animals from NZBW-CAP died before the euthanasia procedure. No deaths occurred on C57-FA, C57-CAP and NZBW-FA groups ($p = 0.007$) (Fig. 2).

Body weight

Both NZBW-FA and NZBW-CAP groups presented a higher body weight when compared to both C57-FA and C57-CAP groups during the whole period ($p < 0.010$). However, comparing animals of same strain, there were no differences between groups exposed to FA or CAP (Fig. 3).

Figure 3: Body weight (g) during the period of exposure to FA or CAP. Bars represent mean ± standard error. n = 8–10 animals/group. *$p < 0.01$ when compared to both C57-FA and C57-CAP (ANOVA followed by post-hoc test Gabriel or Games-Howell). C57-FA: control-filtered; C57-CAP: control-pollution; NZBW-FA: lupus-filtered; NZBW-CAP: lupus-pollution.

Weight of organs

In regarding to absolute weight of organs, NZBW-FA and NZBW-CAP groups presented increased values when compared to C57-FA and C57-CAP groups for kidney ($p < 0.001$), liver ($p < 0.001$) and heart ($p < 0.001$). Kidney weight was higher in NZBW-CAP when compared to NZBW-FA ($p = 0.025$). Spleen weight was higher in NZBW-CAP when compared to C57-FA ($p = 0.027$) and NZBW-FA ($p = 0.046$). Thymus weight was higher in NZBW-CAP and C57-FA groups when compared to C57-CAP ($p = 0.006$; $p = 0.011$) and NZBW-FA ($p = 0.006$; $p = 0.011$) (Table 2). NZBW-FA group presented lower relative weight of all organs (kidney ($p < 0.001$), spleen ($p = 0.006$), liver ($p < 0.001$), heart ($p = 0.042$) and thymus ($p < 0.001$)) when compared to C57-FA group. Except for the liver ($p = 0.052$) and the heart ($p = 0.099$), NZBW-CAP group presented higher relative weights of organs when compared to NZBW-FA group (kidney ($p < 0.001$), spleen ($p = 0.029$) and thymus ($p = 0.007$)) (Table 2).

Table 2
Weight of organs (absolute and relative).

		C57-FA	C57-CAP	NZBW-FA	NZBW-CAP
Absolute (g)	Kidney	0.153 ± 0.008	0.162 ± 0.024	$0.203 \pm 0.014^{a,b}$	$0.263 \pm 0.040^{a,b,c}$
	Spleen	0.082 ± 0.008	0.084 ± 0.015	0.094 ± 0.027	$0.173 \pm 0.124^{a,c'}$
	Liver	1.127 ± 0.107	1.080 ± 0.197	$1.549 \pm 0.137^{a,b}$	$1.807 \pm 0.488^{a,b}$
	Heart	0.104 ± 0.004	$0.120 \pm 0.015^{a'}$	$0.157 \pm 0.014^{a,b}$	$0.177 \pm 0.041^{a,b}$
	Thymus	0.091 ± 0.020	0.057 ± 0.019^{a}	0.059 ± 0.013^{a}	$0.106 \pm 0.045^{b,c}$
Relative (%)	Kidney	0.66 ± 0.05	0.66 ± 0.06	$0.53 \pm 0.04^{a,b}$	0.73 ± 0.17^{c}
	Spleen	0.35 ± 0.02	0.34 ± 0.04	$0.24 \pm 0.07^{a,b}$	$0.45 \pm 0.26^{c'}$
	Liver	4.87 ± 0.39	$4.36 \pm 0.61^{a'}$	4.06 ± 0.29^{a}	4.88 ± 0.94
	Heart	0.45 ± 0.03	0.49 ± 0.06	$0.41 \pm 0.03^{a,b}$	0.48 ± 0.10
	Thymus	0.39 ± 0.08	0.23 ± 0.08^{a}	0.15 ± 0.03^{a}	$0.28 \pm 0.09^{a,c}$

Values represented by mean ± standard deviation. n = 7–10 animals/group. ANOVA followed by post-hoc test Gabriel or Games-Howell or T-test.

$^{a,a'}$ $p < 0.05$ when compared to C57-FA (^{a} ANOVA; $^{a'}$ T-test).

^{b} $p < 0.05$ when compared to C57-CAP.

$^{c,c'}$ $p < 0.05$ when compared to NZBW-FA (^{c} ANOVA; $^{c'}$ T-test).

C57-FA: control-filtered; C57-CAP: control-pollution; NZBW-FA: lupus-filtered; NZBW-CAP: lupus-pollution.

Detection of anti-DNA antibodies

Semi-quantitative analysis of anti-DNA showed that only NZBW animals had a positive reaction. NZBW-FA presented 10% of positivity and NZBW-CAP presented 14.29%. However, there were no statistical differences between groups.

Hemogram

There were no differences in the number of erythrocytes between groups. NZBW-FA group presented a decreased number of total leukocytes (p = 0.018) and lymphocytes (p = 0.006) when compared to C57-FA group. NZBW-CAP group presented an increased number of neutrophils (p = 0.017) when compared to NZBW-FA group. Also, when compared to all other groups, NZBW-CAP presented a decreased percentage of lymphocytes (C57-FA (p < 0.001), C57-CAP (p = 0.002), NZBW-FA (p = 0.018)), and an increased percentage of neutrophils (C57-FA (p = 0.001), C57-CAP (p = 0.002), NZBW-FA (p = 0.016)). The number of platelets was lower in NZBW-FA group when compared to C57-CAP group (p = 0.037) (Table 3).

Table 3
Hemogram analysis of erythrocytes, platelets and leukocytes (total, neutrophils, lymphocytes and monocytes)

	C57-FA	C57-CAP	NZBW-FA	NZBW-CAP
Erythrocytes[1]	9.43 ± 0.30	8.71 ± 0.62	10.39 ± 1.89	7.90 ± 2.03
Platelets[2]	1119.2 ± 115.8	1334.3 ± 396.6	664.8 ± 368.2[b]	684.0 ± 307.0
Leukocytes[2]	3.34 ± 0.96	2.70 ± 0.59	1.72 ± 0.51[a]	2.70 ± 0.66
Lymphocytes[2]	2.54 ± 0.74	2.00 ± 0.32	1.20 ± 0.40[a]	1.50 ± 0.31
Neutrophils[2]	0.71 ± 0.24	0.67 ± 0.28	0.50 ± 0.15	1.13 ± 0.31[c]
Monocytes[2]	0.09 ± 0.08	0.03 ± 0.01	0.02 ± 0.01	0.06 ± 0.06
Lymphocytes (%)	76.00 ± 5.05	74.75 ± 5.12	69.40 ± 5.86	56.00 ± 2.65[a,b,c]
Neutrophils (%)	21.40 ± 3.91	24.00 ± 5.35	29.40 ± 5.81	41.67 ± 1.53[a,b,c]
Monocytes (%)	2.60 ± 1.67	1.25 ± 0.50	1.20 ± 0.45	2.00 ± 1.73
Values represented by mean ± standard deviation. [1](million/mm³); [2](thousand/mm³). n = 3–5 animals/group. ANOVA followed by post-hoc test Gabriel.				
[a] p < 0.05 when compared to C57-FA				
[b] p < 0.05 when compared to C57-CAP				
[c] p < 0.05 when compared to NZBW-FA				
C57-FA: control-filtered; C57-CAP: control-pollution; NZBW-FA: lupus-filtered; NZBW-CAP: lupus-pollution.				

Proteinuria

PCR was followed during the whole period of exposure (from month 0 to month 4). At month 0, NZBW-FA (p < 0.001), NZBW-CAP (p < 0.001) and C57-CAP (p = 0.002) presented decreased PCR when compared to C57-FA. NZBW-FA maintained a lower PCR when compared to C57-FA at month 1 (p = 0.045) and month 2 (p = 0.003). NZBW- CAP presented increased PCR when compared to NZBW-FA at month 2 (p = 0.001), month 3 (p = 0.006) and month 4 (p = 0.034). NZBW-CAP also presented increased PCR when compared to C57-CAP at month 3 (p =

0.046) and month 4 ($p < 0.001$). At month 4, NZBW-FA presented higher PCR when compared to C57-CAP ($p = 0.021$), and NZBW-CAP presented increased PCR when compared to C57-FA ($p = 0.001$) (Fig. 4). ACR was performed with urine collected at the day of euthanasia. There were no differences between the groups.

Stereology of kidneys

Fractional volume of kidney major compartments estimated by Cavalieri principle showed that C57-CAP ($p = 0.035$) and NZBW-CAP ($p = 0.032$) groups presented an increase in the volume of cortex when compared to C57-FA group, and C57-CAP presented a decrease in the volume of medulla when compare to C57-FA ($p = 0.021$) (Fig. 5A). In absolute volume analysis, NZBW-FA group presented a larger volume of cortex when compared to C57-FA ($p = 0.001$) and NZBW-CAP group presented a larger volume of cortex when compared to all the other groups (C57-FA ($p < 0.001$); C57-CAP ($p < 0.001$); NZBW-FA ($p = 0.034$)) (Fig. 5B).

Figure 5: Stereological analysis of kidneys for estimation of fractional (A) and absolute (B) volumes of kidney compartments. Bars represent mean ± standard error. n = 5–6 animals/group. *$p < 0.05$ (ANOVA followed by post-hoc test Gabriel or Games-Howell). C57-FA: control-filtered; C57-CAP: control-pollution; NZBW-FA: lupus-filtered; NZBW-CAP: lupus-pollution.

Histopathology of kidneys

In histopathological analysis of the renal tubules, both NZBW-FA ($p = 0.044$) and NZBW-CAP ($p = 0.005$) groups presented a higher score when compared to C57-FA (Fig. 6A). Glomerular evaluation indicated a higher score in NZBW-CAP when compared to C57-FA ($p = 0.003$) and C57-CAP ($p = 0.025$). Also, NZBW-FA presented a higher score when compared to C57-FA ($p = 0.001$) and C57-CAP ($p = 0.010$) (Fig. 6B). No differences between the groups were observed regarding the mean volume of glomeruli.

Picrosirius analysis

There were no differences between the groups in the fractional area positively stained with picrosirius, indicating fibrosis.

Immunohistochemistry

Deposition of C3 complement positively marked with DAB presented no differences between the groups. We observed a tendency to increased deposition of IgG in NZBW mice, without differences between NZBW-FA and NZBW-CAP groups (Fig. 7). Macrophage quantification was significantly higher in NZBW-FA ($p = 0.023$) and NZBW-CAP ($p = 0.007$) groups in comparison to C57-FA group and, NZBW-CAP presented an increase when compared to C57-CAP group ($p = 0.028$). However, no differences were observed between NZBW-FA and NZBW-CAP groups (Fig. 8).

Gene expression

Gene expression of NF-κB was lower in C57-CAP group when compared to C57-FA ($p = 0.010$) and NZBW-CAP ($p = 0.032$) groups (Fig. 9A). TGF-β expression was higher in C57-FA when compared to NZBW-FA ($p = 0.002$) and NZBW-CAP ($p = 0.005$) groups (Fig. 9B). No significant differences were observed between NZBW-FA and NZBW-CAP groups.

Oxidative stress

NADPH oxidase activity was higher in group NZBW-FA when compared to C57-CAP ($p = 0.011$) and a tendency of increase was observed when compared to C57-FA ($p = 0.055$) (Fig. 10A). Dosage of hydrogen peroxide presented no differences between groups (Fig. 10B). FRAP activity was higher in NZBW-FA ($p = 0.048$) and NZBW-CAP ($p = 0.021$) when compared to the control group (C57-FA) (Fig. 10C). No differences were observed between NZBW-FA and NZBW-CAP groups in oxidative stress analyses.

Discussion

Chronic exposure to PM 2.5 leads to the exacerbation of some clinical manifestations of SLE in a murine model of lupus disease (NZBWF1 mice). Different outcomes were evaluated, however the most striking result is the decreased survival rate in lupus prone mice exposed to particulate air pollution and, as expected, increases in kidney weight and renal cortex volume, early proteinuria onset, as well as elevated number of circulating neutrophils.

Autoimmune diseases are very complex diseases and can affect different organs due to loss of self-tolerance and inappropriate activation of the immune system that leads to the production of autoantibodies and generates tissue destruction. Most common autoimmune diseases are: SLE, rheumatoid arthritis, multiple sclerosis and type 1 diabetes [10]. The etiopathogenesis of these diseases are still under investigation, but there is evidence that in addition to a genetic predisposition, environmental factors may contribute to the onset and worsening of these diseases [8]. Recent epidemiological studies clearly show an association between air pollution and disease activity in patients with SLE. However, there is no agreement of which of the pollutants are most associated to the outcomes and possibly they differ due to the occurrence of the disease is strongly related to race, gender and age [43, 44, 45, 46]. Furthermore, in vitro studies showed that PM can induce T lymphocyte activation, thus contributing to the aggravation of autoimmune diseases [47, 48].

Despite the methodological differences between epidemiological and in vitro studies, all of them corroborates our results that exposure to particulate air pollution exacerbates SLE manifestations in NZBW mice.

To our knowledge, this is the first study that investigated the effects of exposure to “real world” urban particulate air pollution (whole-body inhalation) on lupus-prone animals, a model that mimics some clinical manifestations of SLE in humans. NZBW mice were chosen as SLE animal model based on literature descriptions, since it is considered as the classic model of SLE [49, 50]. Furthermore, only females were utilized in order to mimic disease prevalence in humans (90% of adult patients are women) [2].

The onset of SLE manifestations in female NZBW mice occurs around 28-week-old (7-month-old) and average lifespan is 245 days [51]. We planned our experimental design following this characteristic, thus exposures started 4 months before the expected onset of the clinical manifestations, in order to check if air pollution could anticipate the symptoms. Although not expected, lupus-prone mice presented a significant reduction in life expectancy (less 25%) due to exposure to air pollution. Globally, different studies have already shown that air pollution leads to reductions in life expectancy [52, 53, 54]. However, to date there is no data on mortality risk for SLE patients.

Previous studies using a different mice model for SLE (New Zealand Mixed, NZM), have shown that instillation of silica particles increased mortality due to renal complications [55] and instillation of particulate matter (PM1648 and PM2.5, dose 500 μg) also increased mortality of NZM, but with absence of renal impairments [56]. In our model, NZBW mice exposed to CAP presented early development of proteinuria and the weight of the kidney was increased compared to NZBW exposed to FA, although histopathological scores, fibrosis and C3 complement deposition on kidneys were not different between these groups, and premature death was probably caused by renal failure.

Detection of anti-DNA in serologic tests is important for confirmation of SLE diagnosis [57]. Usually, experimental studies perform anti-DNA quantification assays for evaluation of disease activity [58, 59]. As observed in previous studies with SLE-prone mice exposed to silica [55, 60, 61], we had expected an increase in detection of anti-DNA antibodies in NZBW group exposed to PM2.5. However, there were no differences between the groups. Two aspects can explain this difference: evaluation at the end of the experiment and not during the course and the low number of animals assessed. Anti-DNA antibodies participate in pathogenesis of renal lesions, but its relationship with disease activity and severity varies. Goulart and colleagues showed association between anti-DNA and renal impairments in children [46]. Other studies failed to show a clear correlation between circulating anti-DNA and the type or severity of renal disease in individual patients [62, 63].

In general, SLE patients are prone to the development of hematologic alterations such as anemia, leucopenia and thrombocytopenia, associated with symptoms such as fatigue and susceptibility to infections [64]. In the current study, we observed that NZBW-FA group presented leucopenia and thrombocytopenia, following conditions observed in human patients [57]. We did not observe differences between FA and CAP groups in erythrocytes and platelets counts; however, leukocytes were altered. Female NZBW mice exposed to CAP presented increased percentage and total number of neutrophils and decreased percentage of lymphocytes when compared to NZBW-FA group. Interestingly, neutrophil/lymphocyte ratio can be considered a biomarker associated with increased SLE activity [65]. Thus, exposure to PM2.5 induced negative impacts on the blood of female NZBW mice.

Exposure to PM2.5 also impacted the weight of organs on SLE-prone mice. Body weight did not vary, however NZBW mice exposed to PM2.5 presented higher weight of organs compared to NZBW-FA group. Increase in weight of lymphoid organs such as thymus and spleen can be associated with systemic condition of increased disease activity, characterized by hyperplasia of lymphoid follicles present in these organs [66, 67]. Increase in weight of liver is frequently associated with splenomegaly in SLE patients, however the mechanisms involved are not elucidated [68]. Increased renal weight is associated with a worse renal histopathology [69]. SLE inflammation processes caused by deposition of immune complexes, cell infiltration and formation of lymphoid structures in hepatic and renal parenchyma [70, 71] can be associated with these outcomes, although no significant differences were observed in the histopathological evaluation of the kidneys.

Morphometric evaluation of the kidney structure revealed that in NZBW mice exposed to CAP, the renal cortex volume was increased compared to FA group. These changes were accompanied by altered kidney function (augmented proteinuria). Increase of renal cortex can be related to hypertrophy of nephrons, characterized by large glomeruli and dilated tubules [72]. This condition is associated with increased glomerular filtration rate and, frequently, proteinuria [72, 73]. Nephron hypertrophy can occur by compensatory mechanisms when nephrons are lost due to disease progression, however this condition impairs glomerular function over time [74,

75]. NZBW descriptions show the appearance of proteinuria around 5 to 7 months-age in females [51]. In this current study, NZBW animals exposed to CAP presented an earlier onset of proteinuria when compared to NZBW-FA group, with progression starting at month 2 (5-month-age) and intensified at month 3 (6-month-age) and month 4 (7-month-age). Although proteinuria appeared early on NZBW exposed to CAP, we did not observe a significant increase in the mean volume of glomeruli. Whether the increase of renal cortex can be influenced by interstitial enlargement remains to be determined.

Deposition of collagen and complement proteins, markers of fibrosis and immune complexes deposition on kidneys, respectively, did not differ between groups. Other lesions such as basal membrane thickening, mesangial cell expansion and inflammation, that are characteristic of kidney injury in lupus nephritis [22], were more pronounced in NZBW strain, however exposure to PM2.5 did not exert influence on exacerbation of lesions that could corroborate the outcomes of kidney weight increase and proteinuria development.

Some epidemiological studies reported impairment of renal function on SLE patients exposed to PM2.5. Children diagnosed with SLE and inhabitants of São Paulo city presented increased proteinuria, leukocyturia and hematuria following an increase in PM2.5 concentrations [46]. In the same way, adult patients diagnosed with SLE presented renal complications associated with exposure to PM2.5 in the city of Montreal, Canada [76]. Furthermore, risk of nephropathies, including lupus nephritis, were associated with long term exposure to air pollutants in China [77]. Regarding to animal models of SLE, no kidney alterations were observed in a study that treated NZM mice with instilled PM [56]. On the other hand, studies with silica particles demonstrated kidney impairments with development of proteinuria and renal histopathologic alterations in lupus-prone mice instilled with silica solutions [55, 60].

In brief, our data indicate that exposure to particulate air pollution aggravates and anticipates the disease progression, renal function is compromised, however the mechanisms involved are not clear. Based on previous suggestions, we expected that oxidative stress together with an increase in the complement deposition and augmented inflammatory response would explain the association between air pollution and kidney impairments [78, 79]. However, analysis showed no differences between groups in NF-κB and TGF-β expressions or in the balance of pro/antioxidant molecules.

Conclusions

Despite the variability among the NZBW strain regarding to the development of disease manifestations, negative effects of air pollution in SLE-prone mice is evident, corroborating findings from epidemiological studies. Taking together, our results show that inhalation of CAP induces alterations on clinical manifestations of female NZBW. Complementary studies are important for a better elucidation of the association between air pollution and SLE and the physiopathological mechanisms involved. Reduction of air pollution levels is needed in order to provide a better quality of life for individuals diagnosed with SLE.

Abbreviations

ACR: albumin/creatinine ratio; CAP: concentrated ambient particles; CEUA: Ethical Committee for Animal Research; DAB: 3,3'-diaminobenzidine; EDX: energy dispersive X-ray spectroscopy; FA: filtered air; FMUSP: School of Medicine of University of São Paulo; FRAP: ferric reducing antioxidant power; HAPC: Harvard Ambient Particle

Concentrator; HE: hematoxylin-eosin; IC: immune complexes; PAS: periodic acid-Schiff; PM2.5: fine particulate matter; PCR: protein/creatinine ratio; SLE: systemic lupus erythematosus; WHO: World Health Organization.

Declarations

Ethics approval and consent to participate: Animal procedures were approved by the Ethical Committee for Animal Research (CEUA) of the School of Medicine of University of São Paulo (FMUSP), under protocol number 095/17.

Consent for publication: Not applicable.

Availability of data and materials: All the data that support the findings of this study are available on request from the corresponding author.

Competing interests: The authors declare that they have no competing interests.

Funding: This work was supported by the São Paulo Research Foundation (FAPESP) [grant numbers 2018/05187-5, 2017/05264-7]; the School of Medicine Foundation (FFM) [grant number CG 83.480]; and the Coordenação de Aperfeiçoamento de Pessoal de Nível Superior – Brasil (CAPES) [Finance Code 001].

Authors' contributions: VYY: Conceptualization, Methodology, Validation, Formal analysis, Investigation, Writing (original draft, review and editing), Visualization, Funding acquisition. JIT: Investigation. ARPS: Validation, Investigation, Writing (review and editing). SCFF: Investigation, Writing (review and editing). KA: Validation, Resources; SCLF: Conceptualization, Methodology, Validation, Writing (review and editing), Supervision. NOSC: Methodology, Validation, Resources, Writing (review and editing), Supervision, Funding acquisition. MMV: Conceptualization, Methodology, Validation, Resources, Writing (original draft, review and editing), Supervision, Project administration, Funding acquisition. All authors read and approved the final manuscript.

Acknowledgements: We would like to thank Ivone Oliveira, Marcos Cenedeze, Margarete Vendramini, Meire Hiyane, Nathalia Villa and Regiani Carvalho for technical support and Patricia Prada, Luiz Rizzo and Paulo Saldiva for support with animals and equipments.

References

1. Tsokos GC. Systemic Lupus Erythematosus. N Engl J Med. 2011;365(22):2110–21. https://doi.org/10.1056/nejmra1100359.
2. Carter EE, Barr SG, Clarke AE. The global burden of SLE: prevalence, health disparities and socioeconomic impact. Nat Rev Rheumatol. 2016;12(10):605–20. https://doi.org/10.1038/nrrheum.2016.137.
3. Lisnevskaia L, Murphy G, Isenberg D. Systemic lupus erythematosus. Lancet. 2014;384(9957):1878–88. https://doi.org/10.1016/s0140-6736(14)60128-8.
4. Parks CG, Santos ASE, Barbhaiya M, Costenbader KH. Understanding the role of environmental factors in the development of systemic lupus erythematosus. Best Pract Res Clin Rheumatol. 2017;31(3):306–20. https://doi.org/10.1016/j.berh.2017.09.005.

5. Ghodke-Puranik Y, Niewold TB. Immunogenetics of systemic lupus erythematosus: a comprehensive review. J Autoimmun. 2015;64:125–36. https://doi.org/10.1016/j.jaut.2015.08.004.
6. Mohan C, Putterman C. Genetics and pathogenesis of systemic lupus erythematosus and lupus nephritis. Nat Rev Nephrol. 2015;11(6):329–41. https://doi.org/10.1038/nrneph.2015.33.
7. Ritz SA. Air pollution as a potential contributor to the 'epidemic' of autoimmune disease. Med Hypotheses. 2010;4(1):110–7. https://doi.org/10.1016/j.mehy.2009.07.033.
8. Barbhaiya M, Costenbader KH. Environmental exposures and the development of systemic lupus erythematosus. Curr Opin Rheumatol. 2016;28(5):497–505. https://doi.org/10.1097/BOR.0000000000000318.
9. Leffers HCB, Lange T, Collins C, Ulff-Møller CJ, Jacobsen S. The study of interactions between genome and exposome in the development of systemic lupus erythematosus. Autoimmun Rev. 2019;18(4):382–92. https://doi.org/10.1016/j.autrev.2018.11.005.
10. Zhao CN, Xu Z, Wu GC, Mao YM, Liu LN, Dan YL, et al. Emerging role of air pollution in autoimmune diseases. Autoimmun Rev. 2019;18(6):607–14. https://doi.org/10.1016/j.autrev.2018.12.010.
11. Gilcrease GW, Padovan D, Heffler E, Peano C, Massaglia S, Roccatello D, et al. Is air pollution affecting the disease activity in patients with systemic lupus erythematosus? State of the art and a systematic literature review. Eur J Rheumatol. 2020;7(1):31–4. https://doi.org/10.5152/eurjrheum.2019.19141.
12. WHO (World Health Organization). Ambient air pollution: A global assessment of exposure and burden of disease. Geneva: World Health Organization; 2016.
13. WHO (World Health Organization). Burden of disease from the joint effects of household and ambient Air pollution for 2016. 2018. https://www.who.int/phe/health_topics/outdoorair/databases/AP_jointeffect_BoD_results_March2014.pdf?ua=1. Accessed 08 September 2020.
14. Veras MM, Damaceno-Rodrigues NR, Silva RMG, Scoriza JN, Saldiva PHN, Caldini EG, Dolhnikoff M. Chronic exposure to fine particulate matter emitted by traffic affects reproductive and fetal outcomes in mice. Environ Res. 2009;109(5):536–43. https://doi.org/10.1016/j.envres.2009.03.006.
15. Kelly FJ, Fussell JC. Air pollution and public health: emerging hazards and improved understanding of risk. Environ Geochem Health. 2015;37(4):631–49. https://doi.org/10.1007/s10653-015-9720-1.
16. Thurston GD, Kipen H, Annesi-Maesano I, Balmes J, Brook RD, Cromar K, et al. A joint ERS/ATS policy statement: what constitutes an adverse health effect of air pollution? An analytical framework. Eur Respir J. 2017;49(1):1600419. https://doi.org/10.1183/13993003.00419-2016.
17. Vallero DA. Fundamentals of air pollution: Part I: Foundations of air Pollution. 5th ed. Cambridge: Academic Press; 2014. https://doi.org/10.1016/C2012-0-01172-6.
18. Pope CA III, Ezzati M, Dockery DW. Fine-particulate air pollution and life expectancy in the United States. N Engl J Med. 2009;360(4):376–86. https://doi.org/10.1056/NEJMsa0805646.
19. Pope CA III, Coleman N, Pond ZA, Burnett RT. Fine particulate air pollution and human mortality: 25 + years of cohort studies. Environ Res. 2020;183:108924. https://doi.org/10.1016/j.envres.2019.108924.
20. Pope CA III, Dockery DW. Health effects of fine particulate air pollution: lines that connect. J Air Waste Manag Assoc. 2006;56(6):709–42. https://doi.org/10.1080/10473289.2006.10464485.

21. Losacco C, Perillo A. Particulate matter air pollution and respiratory impact on humans and animals. Environ Sci Pollut Res. 2018;25(34):33901–10. https://doi.org/10.1007/s11356-018-3344-9.
22. Anders HJ, Fogo AB. Immunopathology of lupus nephritis. Semin Immunopathol. 2014;36(4):443 – 59. https://doi.org/10.1007/s00281-013-0413-5.
23. Tsokos GC, Lo MS, Reis PC, Sullivan KE. New insights into the immunopathogenesis of systemic lupus erythematosus. Nat Rev Rheumatol. 2016;12(12):716–30. https://doi.org/10.1038/nrrheum.2016.186.
24. Flores-Mendoza G, Sansón SP, Rodríguez-Castro S, Crispín JC, Rosetti F. Mechanisms of tissue injury in lupus nephritis. Trends Mol Med. 2018;24(4):364–78. https://doi.org/10.1016/j.molmed.2018.02.003.
25. Cooper GS, Gilbert KM, Greidinger EL, James JA, Pfau JC, Reinlib L, Richardson BC, Rose NR. Recent advances and opportunities in research on lupus: environmental influences and mechanisms of disease. Environ Health Perspect. 2008;116(6):695–702. https://doi.org/10.1289/ehp.11092.
26. Farhat SC, Silva CA, Orione MA, Campos LM, Sallum AM, Braga AL. Air pollution in autoimmune rheumatic diseases: a review. Autoimmun Rev. 2011;11(1):14–21. https://doi.org/10.1016/j.autrev.2011.06.008.
27. Lanata CM, Nititham J, Taylor K, Nayak R, Barcellos L, Chung SA, Galanter J, Criswell LA. Residential proximity to highways, DNA methylation and systemic lupus erythematosus. Lupus Sci Med. 2016;3(1):A1–80. https://doi.org/10.1136/lupus-2016-000179.126.
28. Brito JM, Macchione M, Yoshizaki K, Toledo-Arruda AC, Saraiva-Romanholo BM, Andrade MD, et al. Acute cardiopulmonary effects induced by the inhalation of concentrated ambient particles during seasonal variation in the city of Sao Paulo. J Appl Physiol (1985). 2014;117(5):492–9. https://doi.org/10.1152/japplphysiol.00156.2014.
29. Yoshizaki K, Fuziwara CS, Brito JM, Santos TM, Kimura ET, Correia AT, et al. The effects of urban particulate matter on the nasal epithelium by gender: an experimental study in mice. Environ Pollut. 2016;213:359–69. https://doi.org/10.1016/j.envpol.2016.02.044.
30. Di Domenico M, Benevenuto SGM, Tomasini PP, Yariwake VY, Alves NO, Rahmeier FL, et al. Concentrated ambient fine particulate matter (PM2.5) exposure induce brain damage in pre and postnatal exposed mice. Neurotoxicology. 2020;79:127–41. https://doi.org/10.1016/j.neuro.2020.05.004.
31. EPA (Environmental Protection Agency). Exposure Assessment Tools by Routes – Inhalation. 2020. https://www.epa.gov/expobox/exposure-assessment-tools-routes-inhalation. Accessed 24 September 2020.
32. Miranda RM, Andrade MF, Fornaro A, Astolfo R, Andre PA, Saldiva P. Urban air pollution: a representative survey of PM(2.5) mass concentrations in six Brazilian cities. Air Qual Atmos Health. 2012;5(1):63–77. https://doi.org/10.1007/s11869-010-0124-1.
33. Khosho FK, Kaufmann RC, Amankwah KS. A simple and efficient method for obtaining urine samples from rats. Lab Anim Sci. 1985;35(5):513–4.
34. Nyengaard JR. Stereologic methods and their application in kidney research. J Am Soc Nephrol. 1999;10(5):1100–23.
35. Frazier KS, Seely JC, Hard GC, Betton G, Burnett R, Nakatsuji S, et al. Proliferative and nonproliferative lesions of the rat and mouse urinary system. Toxicol Pathol. 2012;40(4):14S–86S. https://doi.org/10.1177/0192623312438736.
36. Lane PH, Steffes MW, Mauer SM. Estimation of glomerular volume: a comparison of four methods. Kidney Int. 1992;41(4):1085–9. https://doi.org/10.1038/ki.1992.165.

37. Montes GS, Junqueira LC. The use of the Picrosirius-polarization method for the study of the biopathology of collagen. Mem Inst Oswaldo Cruz. 1991;86(Suppl 3):1–11. https://doi.org/10.1590/s0074-02761991000700002.
38. Livak KJ, Schmittgen TD. Analysis of relative gene expression data using real-time quantitative PCR and the 2 – ΔΔCT method. Methods. 2001;25(4):402–8. https://doi.org/10.1006/meth.2001.1262.
39. Machi JF, Dias DS, Freitas SC, Moraes OA, Silva MB, Cruz PL, et al. Impact of aging on cardiac function in a female rat model of menopause: role of autonomic control, inflammation, and oxidative stress. Clin Interv Aging. 2016;11:341–50. https://doi.org/10.2147/CIA.S88441.
40. Tietze F. Enzymic method for quantitative determination of nanogram amounts of total and oxidized glutathione: Applications to mammalian blood and other tissues. Anal Biochem. 1969;27(3):502–22. https://doi.org/10.1016/0003-2697(69)90064-5.
41. Pick E, Keisari Y. A simple colorimetric method for the measurement of hydrogen peroxide produced by cells in culture. J Immunol Methods. 1980;38(1–2):161–70. https://doi.org/10.1016/0022-1759(80)90340-3.
42. Benzie IF, Strain JJ. Ferric reducing/antioxidant power assay: direct measure of total antioxidant activity of biological fluids and modified version for simultaneous measurement of total antioxidant power and ascorbic acid concentration. Methods Enzymol. 1999;299:15–27. https://doi.org/10.1016/s0076-6879(99)99005-5.
43. Alves AGF, Giacomin MFA, Braga ALF, Sallum AME, Pereira LAA, Farhat LC, et al. Influence of air pollution on airway inflammation and disease activity in childhood-systemic lupus erythematosus. Clin Rheumatol. 2018;37(3):683–90. https://doi.org/10.1007/s10067-017-3893-1.
44. Jung C, Chung W, Chen W, Lee R, Hwang B. Long-term exposure to traffic-related air pollution and systemic lupus erythematosus in Taiwan: A cohort study. Sci Total Environ. 2019;668:342–9. https://doi.org/10.1016/j.scitotenv.2019.03.018.
45. Zhao C, Mei Y, Wu G, Mao Y, Wu Q, Dan Y, Pan H. Effect of air pollution on hospital admissions for systemic lupus erythematosus in Bengbu, China: a time series study. Lupus. 2019;28(13):1541–8. https://doi.org/10.1177/0961203319882503.
46. Goulart MFG, Alves AGF, Farhat J, Braga ALF, Pereira LAA, Lichtenfels AJFC, et al. Influence of air pollution on renal activity in patients with childhood-onset systemic lupus erythematosus. Pediatr Nephrol. 2020;35(7):1247–55. https://doi.org/10.1007/s00467-020-04517-3.
47. Pierdominici M, Maselli A, Cecchetti S, Tinari A, Mastrofrancesco A, Alfè M, et al. Diesel exhaust particle exposure in vitro impacts T lymphocyte phenotype and function. Part Fibre Toxicol. 2014;11(1):74. https://doi.org/10.1186/s12989-014-0074-0.
48. O'Driscoll CA, Owens LA, Gallo ME, Hoffmann EJ, Afrazi A, Han M, et al. Differential effects of diesel exhaust particles on T cell differentiation and autoimmune disease. Part Fibre Toxicol. 2018;15(1):35. https://doi.org/10.1186/s12989-018-0271-3.
49. Richard ML, Gilkeson G. Mouse models of lupus: what they tell us and what they don't. Lupus Sci Med. 2018;5(1):e000199. https://doi.org/10.1136/lupus-2016-000199.
50. Li W, Titov AA, Morel L. An update on lupus animal models. Curr Opin Rheumatol. 2017;29(5):434–41. https://doi.org/10.1097/BOR.0000000000000412.

51. Hahn BH, Kono D. Dubois' lupus erythematosus and related syndromes: Animal models of SLE. 8th ed. Philadelphia: Saunders; 2013. pp. 190–236. https://doi.org/10.1016/C2010-0-66018-4.
52. Hill TD, Jorgenson AK, Ore P, Balistreri KS, Clark B. Air quality and life expectancy in the United States: An analysis of the moderating effect of income inequality. SSM Popul Health. 2018;7:100346. https://doi.org/10.1016/j.ssmph.2018.100346.
53. Yin P, Brauer M, Cohen AJ, Wang H, Li J, Burnett RT, et al. The effect of air pollution on deaths, disease burden, and life expectancy across China and its provinces, 1990–2017: an analysis for the Global Burden of Disease Study 2017. Lancet Planet Health. 2019;4(9):e386-98. https://doi.org/10.1016/S2542-5196(20)30161-3.
54. Lelieveld J, Pozzer A, Pöschl U, Fnais M, Haines A, Münzel T. Loss of life expectancy from air pollution compared to other risk factors: a worldwide perspective. Cardiovasc Res. 2020;116(11):1910–7. https://doi.org/10.1093/cvr/cvaa025.
55. Brown JM, Archer AJ, Pfau JC, Holian A. Silica accelerated systemic autoimmune disease in lupus-prone New Zealand mixed mice. Clin Exp Immunol. 2003;131(3):415–21. https://doi.org/10.1046/j.1365-2249.2003.02094.x.
56. Hassani M, Brown JM, Morandi MT, Holian A. Particulate matter immunomodulatory effects on autoantibody development in New Zealand mixed mice. J Immunotoxicol. 2004;1(2):95–102. https://doi.org/10.1080/15476910490505644.
57. Aringer M, Costenbader K, Daikh D, Brinks R, Mosca M, Ramsey-Goldman R, et al. 2019 European League Against Rheumatism/American College of Rheumatology Classification Criteria for Systemic Lupus Erythematosus. Arthritis Rheumatol. 2019;71(9):1400–12. https://doi.org/10.1002/art.40930.
58. Bardana EJ Jr, Harbeck RJ, Hoffman AA, Pirofsky B, Carr RI. The prognostic and therapeutic implications of DNA: anti-DNA immune complexes in systemic lupus erythematosus (SLE). Am J Med. 1975;59(4):515–22. https://doi.org/10.1016/0002-9343(75)90259-4.
59. Sohrabian A, Parodis I, Carlströmer-Berthén N, Frodlund M, Jönsen A, Zickert, et al. Increased levels of anti-dsDNA antibodies in immune complexes before treatment with belimumab associate with clinical response in patients with systemic lupus erythematosus. Arthritis Res Ther. 2019;21(1):259. https://doi.org/10.1186/s13075-019-2056-y.
60. Bates MA, Brandenberger C, Langohr I, Kumagai K, Harkema JR, Holian A, Pestka JJ. Silica triggers inflammation and ectopic lymphoid neogenesis in the lungs in parallel with accelerated onset of systemic autoimmunity and glomerulonephritis in the lupus-prone NZBWF1 mouse. PloS One. 2015;10(5):e0125481. https://doi.org/10.1371/journal.pone.0125481.
61. Bates MA, Akbari P, Gilley KN, Wagner JG, Li N, Kopec AK, et al. Dietary docosahexaenoic acid prevents silica-induced development of pulmonary ectopic germinal centers and glomerulonephritis in the lupus-prone NZBWF1 mouse. Front Immunol. 2018;9:2002. https://doi.org/10.3389/fimmu.2018.02002.
62. Okamura M, Kanayama Y, Amatsu K, Negoro N, Kohda S, Takeda T, Inoue T. Significance of enzyme linked immunosorbent assay (ELISA) for antibodies to double stranded and single stranded DNA in patients with lupus nephritis: correlation with severity of renal histology. Ann Rheum Dis. 1993;52(1):14–20. https://doi.org/10.1136/ard.52.1.14.
63. Goilav B, Putterman C. The Role of Anti-DNA Antibodies in the Development of Lupus Nephritis: A Complementary, or Alternative. Viewpoint? Semin Nephrol. 2015;35(5):439–43.

https://doi.org/10.1016/j.semnephrol.2015.08.005.

64. Fayyaz A, Igoe A, Kurien BT, Danda D, James JA, Stafford HA, Scofield RH. Haematological manifestations of lupus. Lupus Sci Med. 2015;2(1):e000078. https://doi.org/10.1136/lupus-2014-000078.
65. Ma L, Zeng A, Chen B, Chen Y, Zhou R. Neutrophil to lymphocyte ratio and platelet to lymphocyte ratio in patients with systemic lupus erythematosus and their correlation with activity: A meta-analysis. Int Immunopharmacol. 2019;76:105949. https://doi.org/10.1016/j.intimp.2019.105949.
66. Nishino M, Ashiku SK, Kocher ON, Thurer RL, Boiselle PM, Hatabu H. The thymus: a comprehensive review. Radiographics. 2016;26(2):335–48. https://doi.org/10.1148/rg.262045213.
67. Zhang Q, Xiang L, Zaman MH, Dong W, He G, Deng GM. Predominant role of immunoglobulin G in the pathogenesis of splenomegaly in murine lupus. Front Immunol. 2020;10:3020. https://doi.org/10.3389/fimmu.2019.03020.
68. Guariento A, Silva MFC, Tassetano PSF, Rocha SMS, Campos LMA, Valente M, Silva CA. Liver and spleen biometrics in childhood-onset systemic lupus erythematosus patients. Rev Bras Reumatol. 2015;55(4):341–51. https://doi.org/10.1016/j.rbr.2014.12.010.
69. Craig EA, Yan Z, Zhao QJ. The relationship between chemical-induced kidney weight increases and kidney histopathology in rats. J Appl Toxicol. 2015;35(7):729–36. https://doi.org/10.1002/jat.3036.
70. Fang X, Zaman MH, Guo X, Ding H, Xie C, Zhang X, Deng GM. Role of hepatic deposited immunoglobulin G in the pathogenesis of liver damage in systemic lupus erythematosus. Front Immunol. 2018;9:1457. https://doi.org/10.3389/fimmu.2018.01457.
71. Sato Y, Boor P, Fukuma S, Klinkhammer BM, Haga H, Ogawa O, Floege J, Yanagita M. Developmental stages of tertiary lymphoid tissue reflect local injury and inflammation in mouse and human kidneys. Kidney Int. 2020;98(2):448–63. https://doi.org/10.1016/j.kint.2020.02.023.
72. Denic A, Alexander MP, Kaushik V, Lerman LO, Lieske JC, Stegall MD, et al. Detection and clinical patterns of nephron hypertrophy and nephrosclerosis among apparently healthy adults. Am J Kidney Dis. 2016;68(1):58–67. https://doi.org/10.1053/j.ajkd.2015.12.029.
73. Elsherbiny HE, Alexander MP, Kremers WK, Park WD, Poggio ED, Prieto M, Lieske JC, Rule AD. Nephron hypertrophy and glomerulosclerosis and their association with kidney function and risk factors among living kidney donors. Clin J Am Soc Nephrol. 2014;9(11):1892–902. https://doi.org/10.2215/CJN.02560314.
74. Kriz W, Lehir M. Pathways to nephron loss starting from glomerular diseases—insights from animal models. Kidney Int. 2005;67(2):404 – 19. https://doi.org/10.1111/j.1523-1755.2005.67097.x.
75. Schnaper HW. The tubulointerstitial pathophysiology of progressive kidney disease. Adv Chronic Kidney Dis. 2017;24(2):107 – 16. https://doi.org/10.1053/j.ackd.2016.11.011.
76. Bernatsky S, Fournier M, Pineau CA, Clarke AE, Vinet E, Smargiassi A. Associations between ambient fine particulate levels and disease activity in patients with systemic lupus erythematosus (SLE). Environ Health Perspect. 2011;119(1):45–9. https://doi.org/10.1289/ehp.1002123.
77. Xu X, Wang G, Chen N, Lu T, Nie S, Xu G, et al. Long-term exposure to air pollution and increased risk of membranous nephropathy in China. J Am Soc Nephrol. 2016;27(12):3739–46. https://doi.org/10.1681/ASN.2016010093.

78. Nemmar A, Karaca T, Beegam S, Yuvaraju P, Yasin J, Hamadi NK, Ali BH. Prolonged pulmonary exposure to diesel exhaust particles exacerbates renal oxidative stress, inflammation and DNA damage in mice with adenine-induced chronic renal failure. Cell Physiol Biochem. 2016;38(5):1703–13. https://doi.org/10.1159/000443109.
79. Busso IT, Mateos AC, Juncos LI, Canals N, Carreras HA. Kidney damage induced by sub-chronic fine particulate matter exposure. Environ Int. 2018;121(Pt1):635–42. https://doi.org/10.1016/j.envint.2018.10.007.

Figures

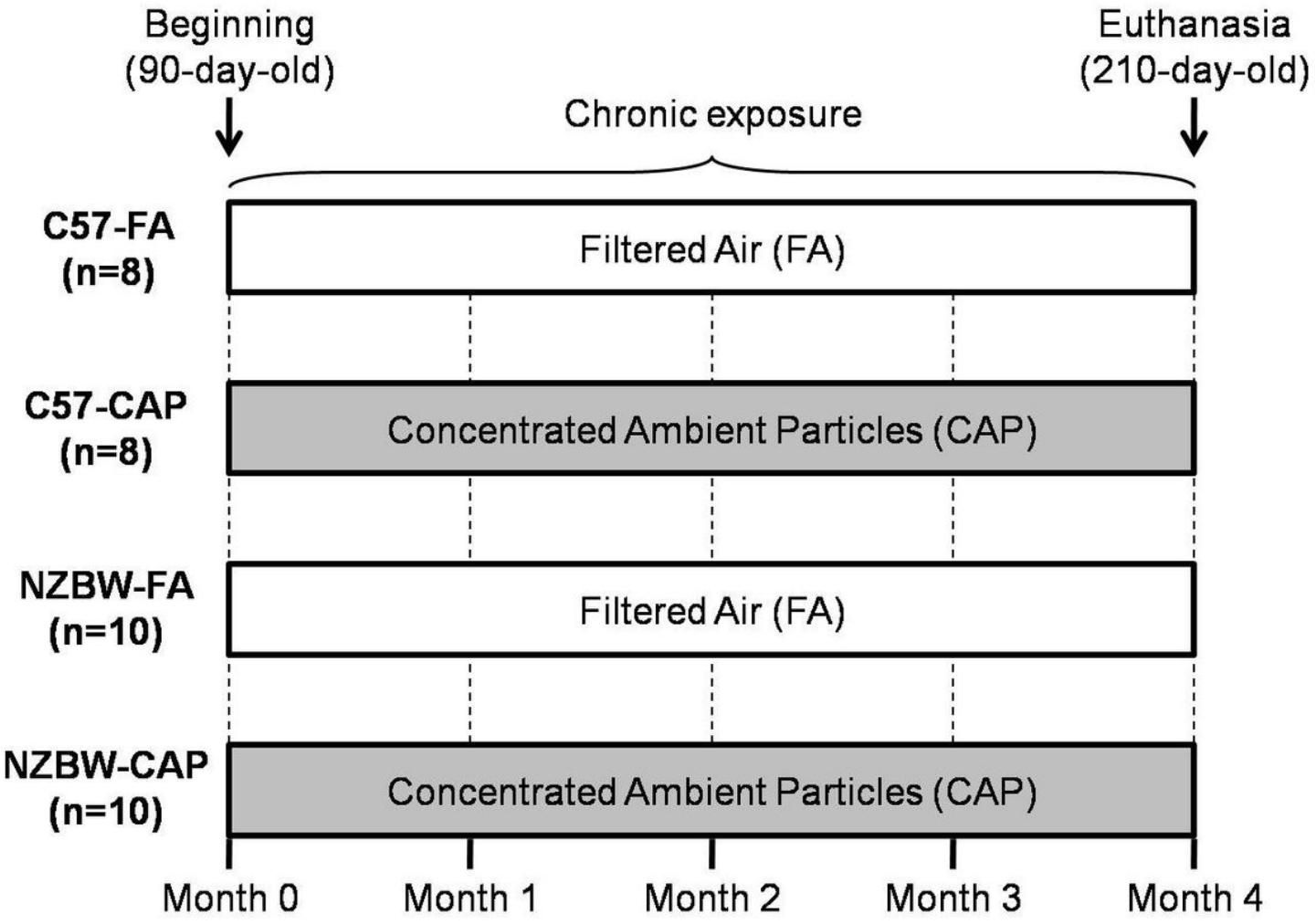

Figure 1

Experimental design. C57-FA: control mice exposed to filtered air; C57-CAP: control mice exposed to concentrated ambient particles (air pollution); NZBW-FA: lupus-prone mice exposed to filtered air; NZBW-CAP: lupus-prone mice exposed to concentrated ambient particles (air pollution).

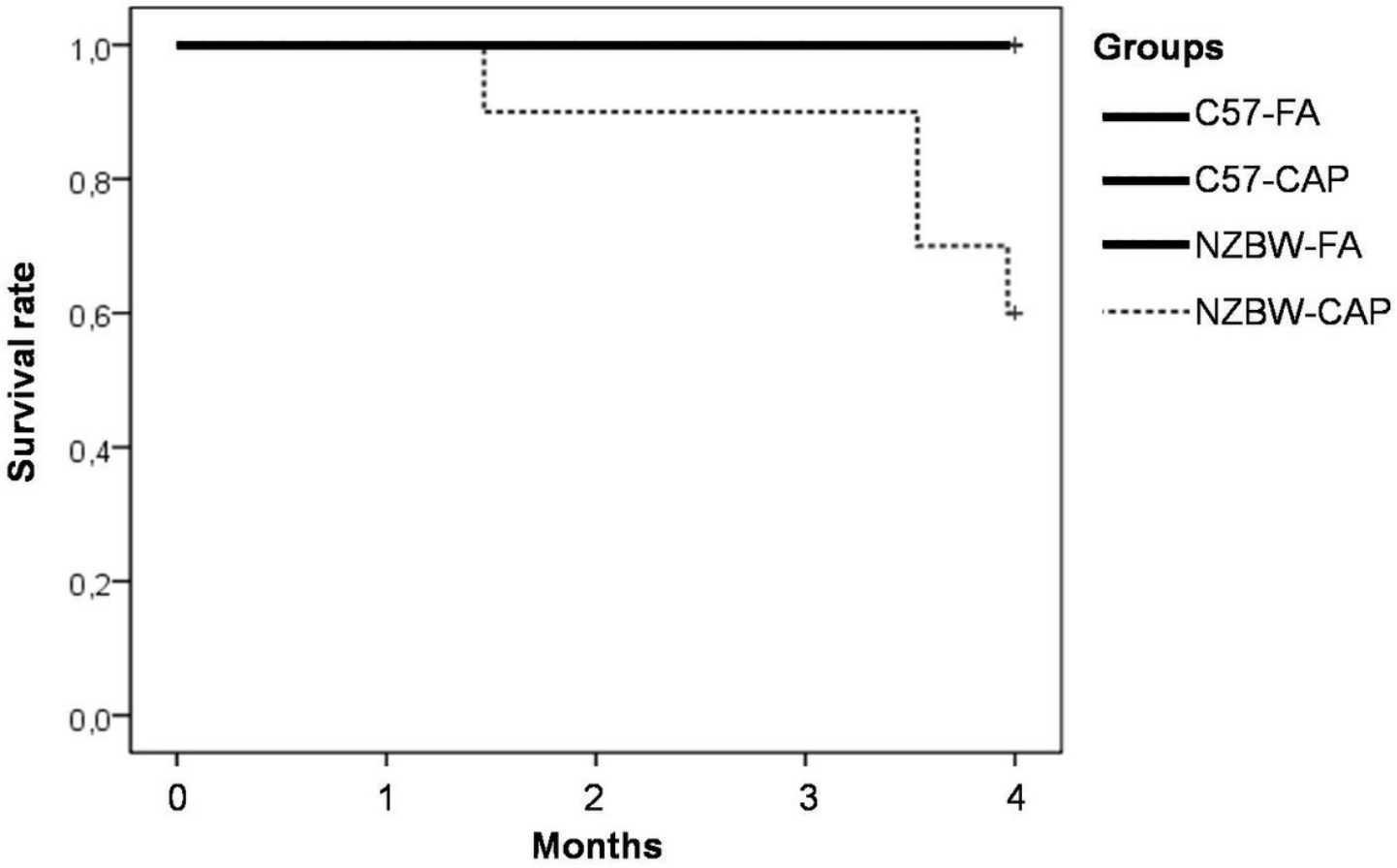

Figure 2

Survival rate during the period of exposure to FA or CAP. n=8-10 animals/group. p=0.007 (Kepler-Meier test). C57-FA: control-filtered; C57-CAP: control-pollution; NZBW-FA: lupus-filtered; NZBW-CAP: lupus-pollution.

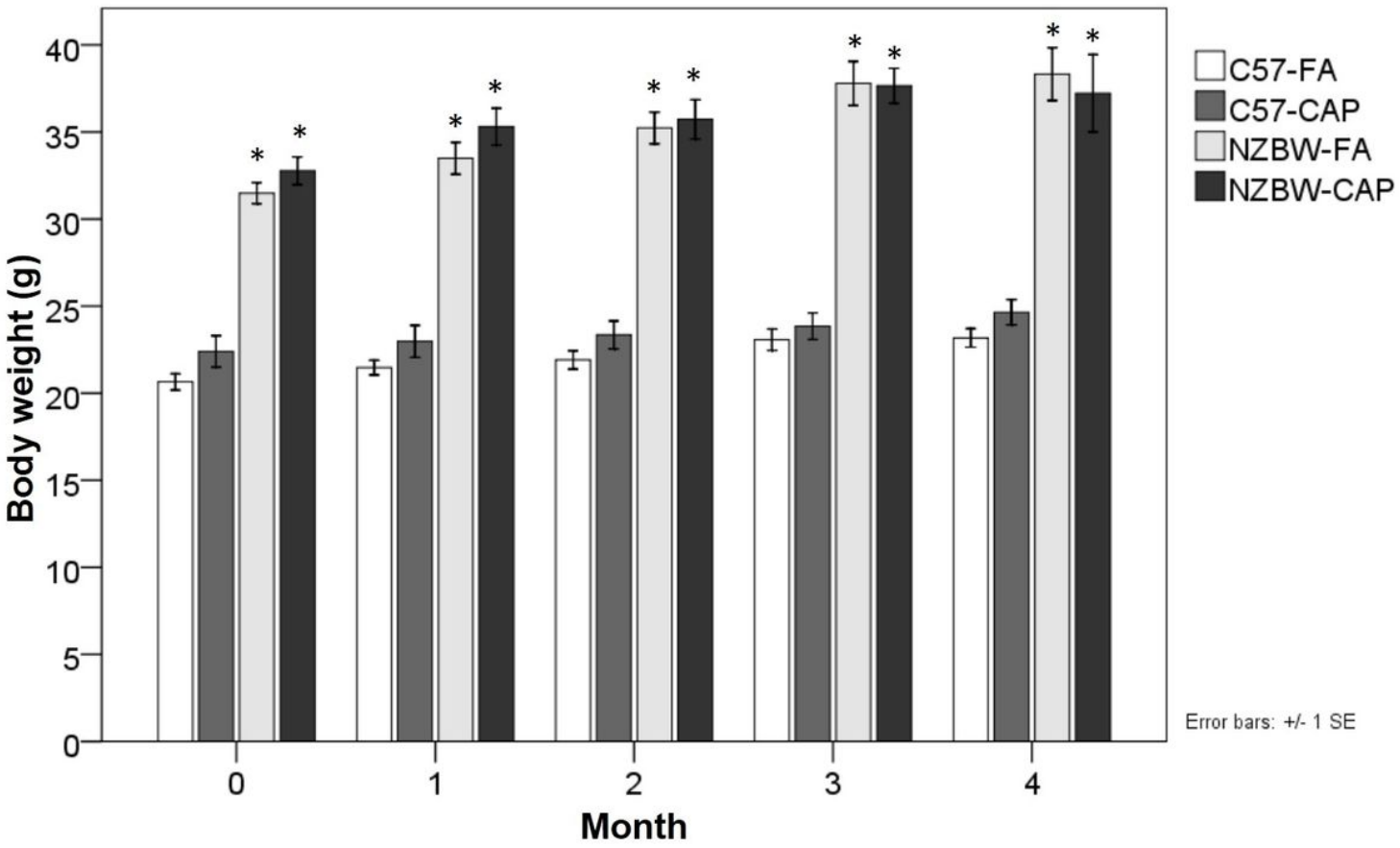

Figure 3

Body weight (g) during the period of exposure to FA or CAP. Bars represent mean ± standard error. n=8-10 animals/group. *p<0.01 when compared to both C57-FA and C57-CAP (ANOVA followed by post-hoc test Gabriel or Games-Howell). C57-FA: control-filtered; C57-CAP: control-pollution; NZBW-FA: lupus-filtered; NZBW-CAP: lupus-pollution.

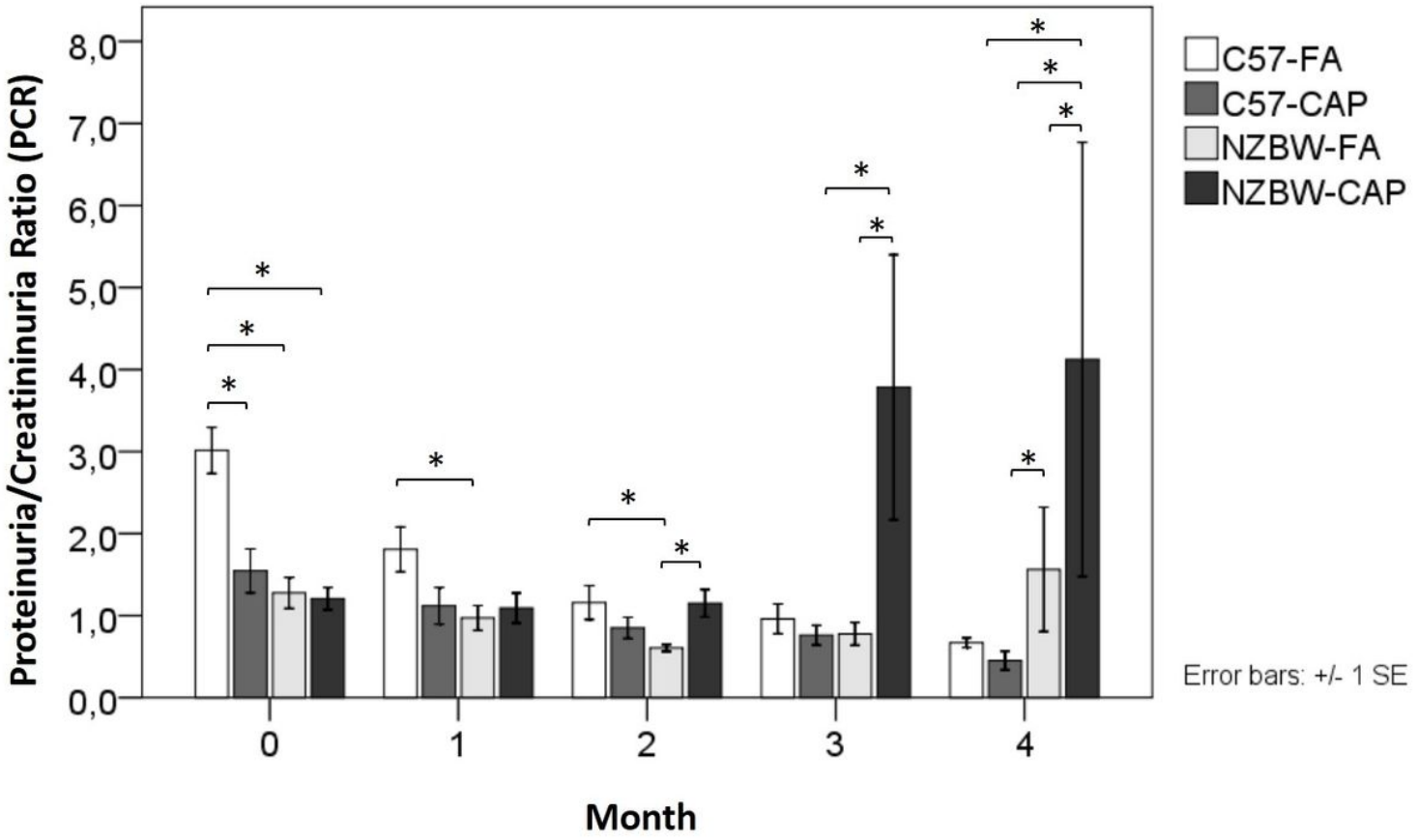

Figure 4

Proteinuria/creatininuria ratio (PCR) during the period of exposure to FA or CAP. Bars represent mean ± standard error. n=5-10 animals/group. *p<0.05 (ANOVA followed by post-hoc test Gabriel). C57-FA: control-filtered; C57-CAP: control-pollution; NZBW-FA: lupus-filtered; NZBW-CAP: lupus-pollution.

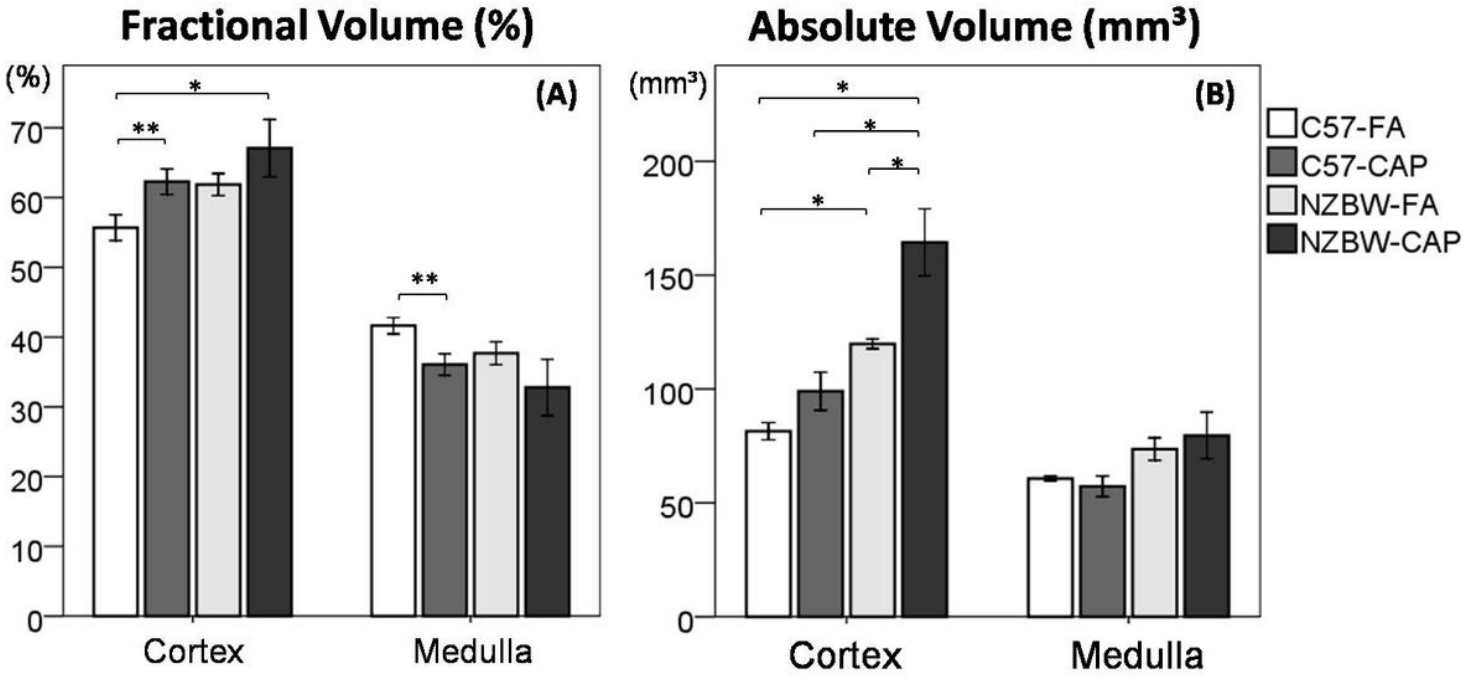

Figure 5

Stereological analysis of kidneys for estimation of fractional (A) and absolute (B) volumes of kidney compartments. Bars represent mean ± standard error. n=5-6 animals/group. *p<0.05 (ANOVA followed by post-hoc test Gabriel or Games-Howell). C57-FA: control-filtered; C57-CAP: control-pollution; NZBW-FA: lupus-filtered; NZBW-CAP: lupus-pollution.

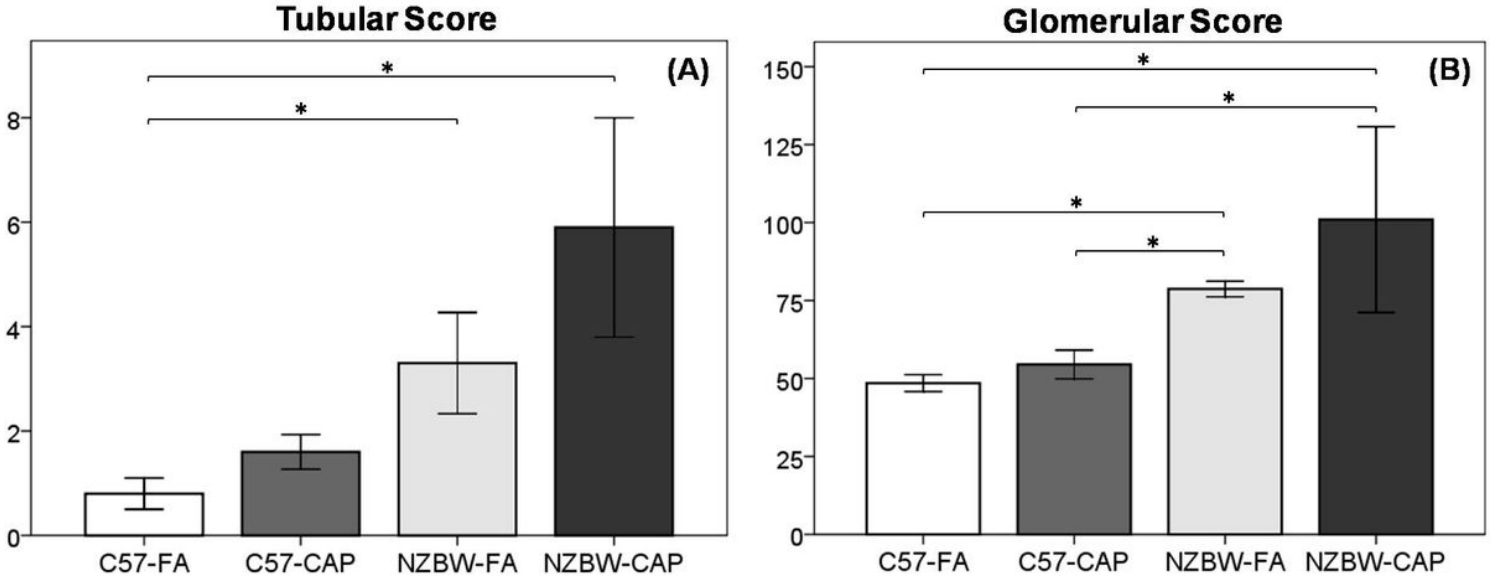

Figure 6

Kidney histopathology (arbitrary units) of tubules (A) and glomeruli (B). Bars represent mean ± standard error. n=5 animals/group. *p<0.05 (ANOVA followed by post-hoc test Tukey HSD). C57-FA: control-filtered; C57-CAP: control-pollution; NZBW-FA: lupus-filtered; NZBW-CAP: lupus-pollution.

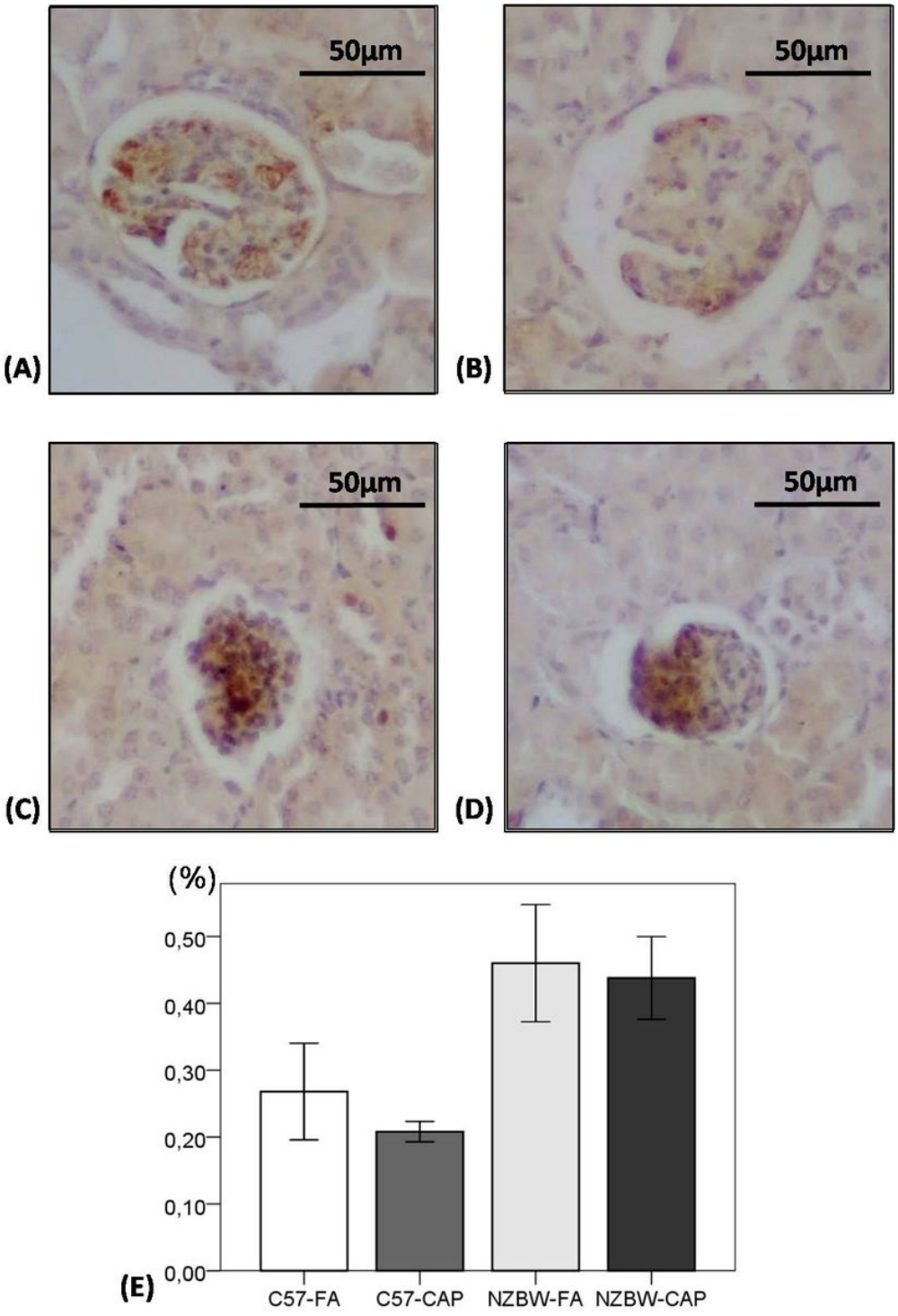

Figure 7

Photomicrographs of kidneys from C57-FA (A), C57-CAP (B), NZBW-FA (C) and NZBW-CAP (D) groups for quantification of IgG deposition (E) by IHC. Bars represent mean ± standard error. n=5-7 animals/group. ANOVA followed by post-hoc test Games-Howell. C57-FA: control-filtered; C57-CAP: control-pollution; NZBW-FA: lupus-filtered; NZBW-CAP: lupus-pollution.

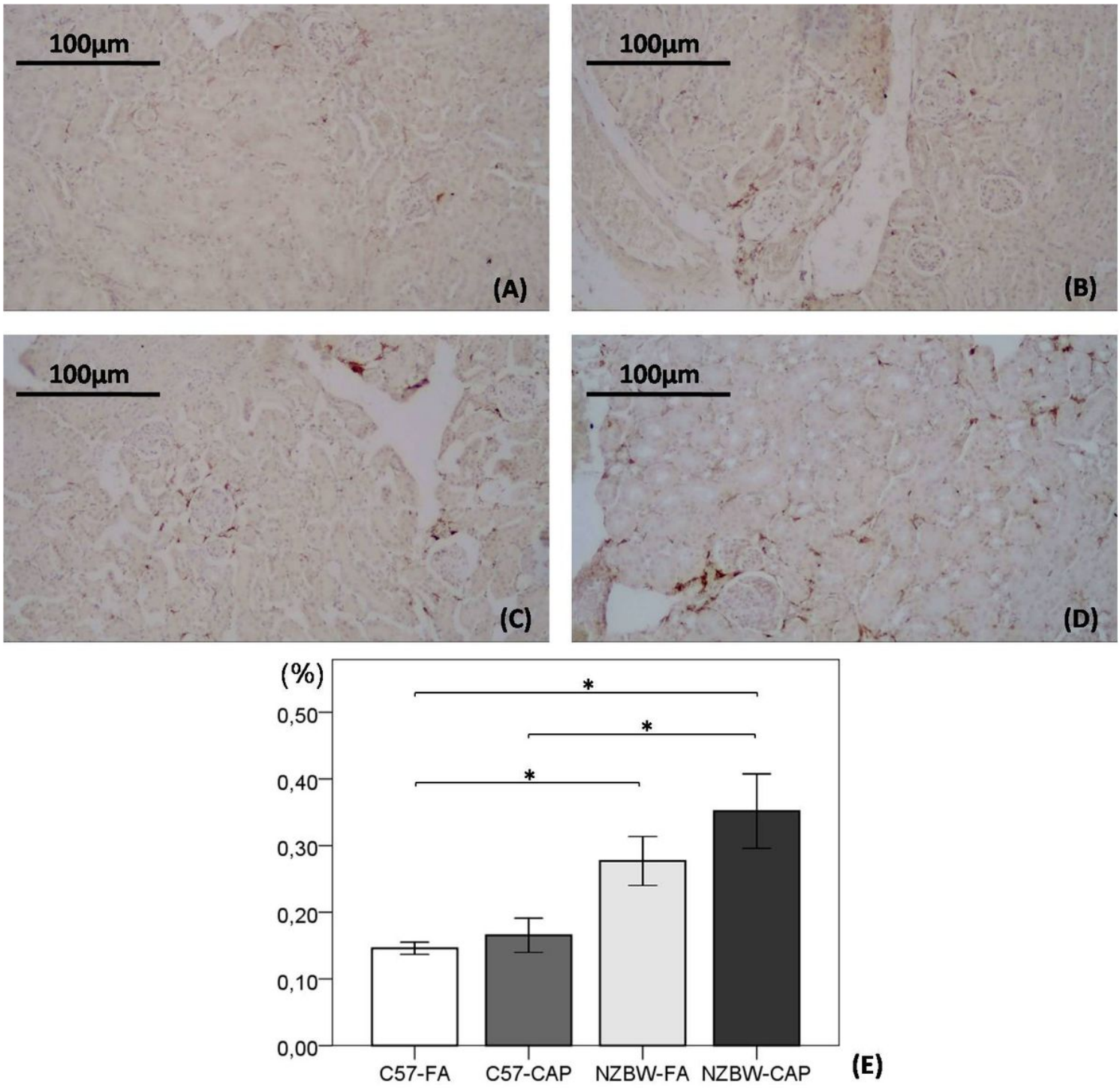

Figure 8

Photomicrographs of kidneys from C57-FA (A), C57-CAP (B), NZBW-FA (C) and NZBW-CAP (D) groups for quantification of macrophages (E) by IHC. Bars represent mean ± standard error. n=5-8 animals/group. *p<0.05 (ANOVA followed by post-hoc test Gabriel). C57-FA: control-filtered; C57-CAP: control-pollution; NZBW-FA: lupus-filtered; NZBW-CAP: lupus-pollution.

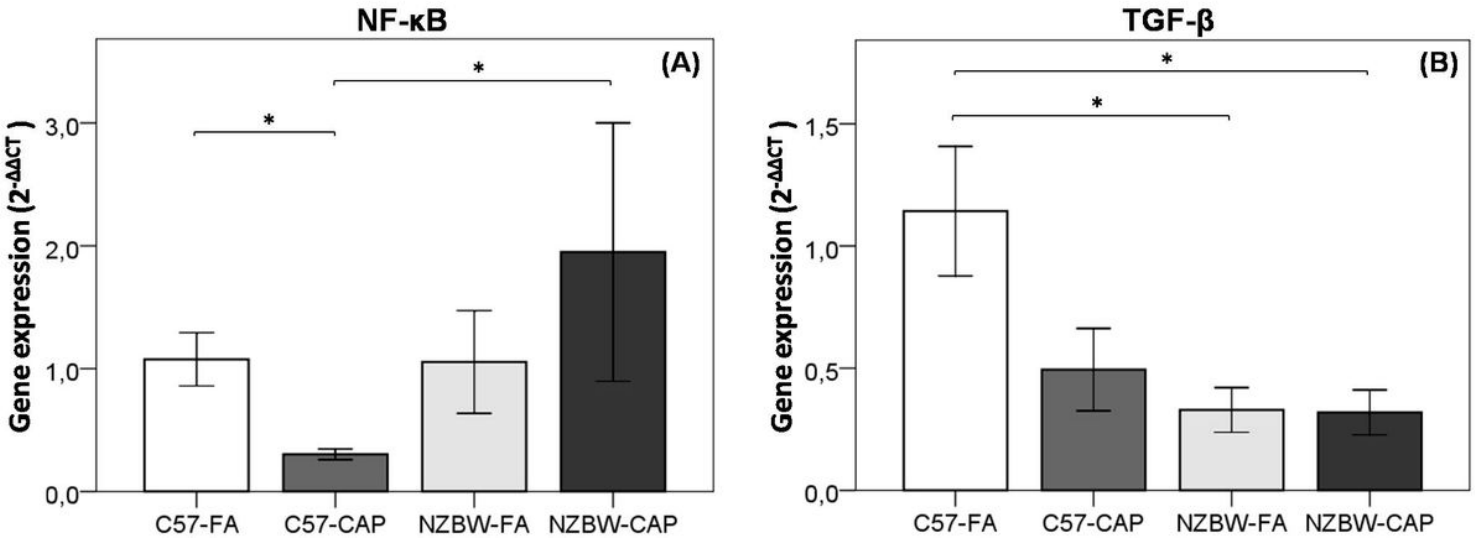

Figure 9

Analysis of gene expression of NF-κB (A) and TGF-β (B) by qRT-PCR. (2-ΔΔCT method). Bars represent mean ± standard error. n=5-10 animals/group. *p<0.05 (ANOVA followed by post-hoc test Gabriel). C57-FA: control-filtered; C57-CAP: control-pollution; NZBW-FA: lupus-filtered; NZBW-CAP: lupus-pollution.

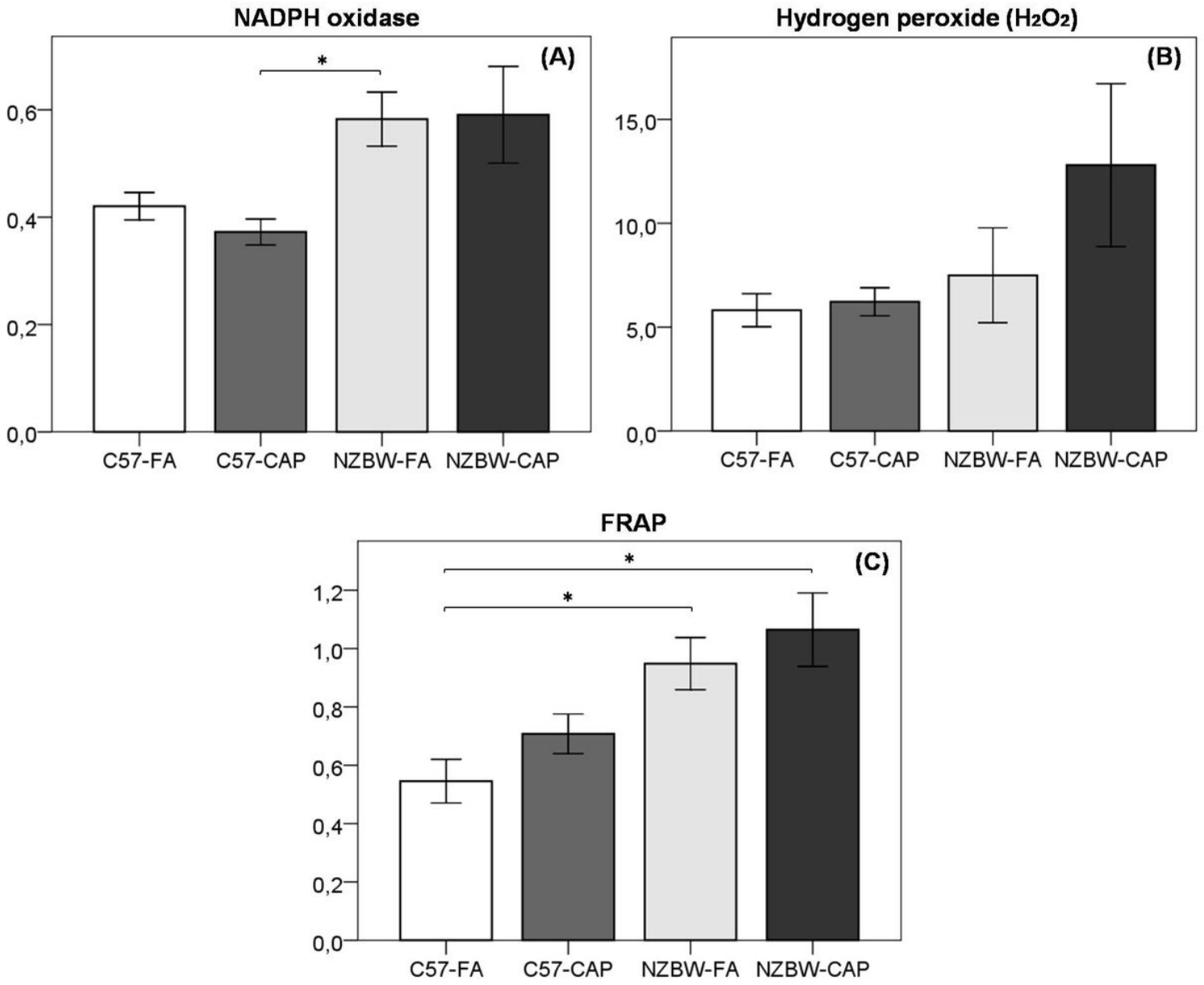

Figure 10

Quantification of NADPH oxidase (A), hydrogen peroxide (B) and ferric reducing antioxidant activity (FRAP) (C) in kidneys. Bars represent mean ± standard error. n=8-10 animals/group. *p<0.05 (ANOVA followed by post-hoc test Gabriel or Games-Howell). C57-FA: control-filtered; C57-CAP: control-pollution; NZBW-FA: lupus-filtered; NZBW-CAP: lupus-pollution.

Supplementary Files

This is a list of supplementary files associated with this preprint. Click to download.

- AdditionalFile1.docx